Electronic Supplementary Material (ESI) for RSC Advances.

Supplementary Information

Computational study of the interaction of the psychoactive amphetamine with 1,2-indanedione and 1,8-diazafluoren-9-one as fingerprinting reagents

D. Bhikharee[1], L. Rhyman[1,2] and P. Ramasami[1,2]*

[1]*Computational Chemistry Group, Department of Chemistry, Faculty of Science, University of Mauritius, Réduit 80837, Mauritius*

[2] *Department of Chemistry, University of South Africa, Private Bag X6, Florida, 1710, South Africa*

*Author for correspondence email: p.ramasami@uom.ac.mu

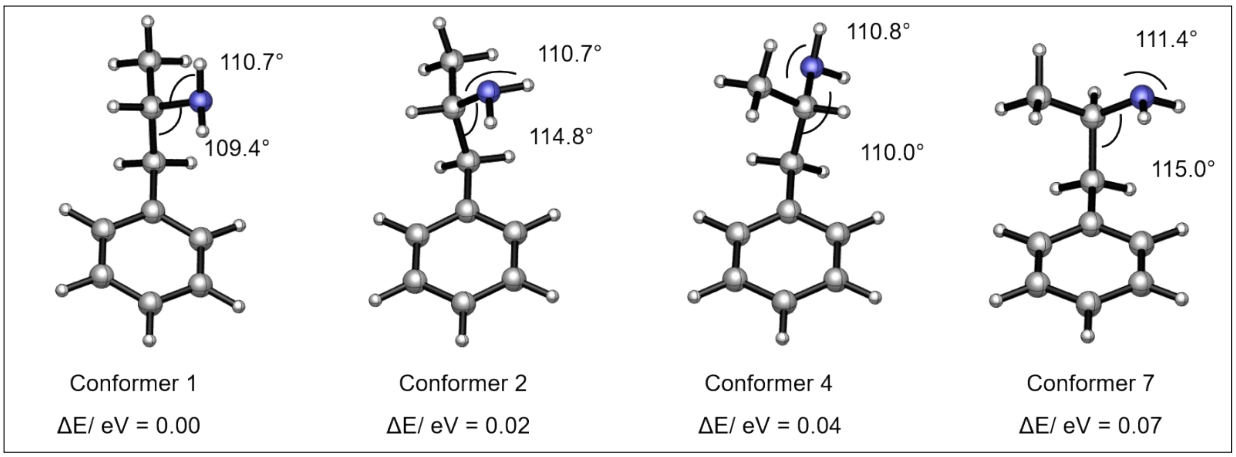

Fig. S1 AMP conformers

Table S1 Interaction angles as indicated by the orange curves in Fig. 3

Structure	Angle between	Angle
AMP-IND	C-O1···H2	69.5
	C-O2···H1	72.9
AMP-DFO	C-N···H1	115.9
	C-O···H2	107.5
ALA-IND	C-H2···O3	96.0
	C-O2···H1	98.9
	C-O1···H1	86.1
ALA-DFO	C-O2···H3	117.5
	C-N···H2	123.7
	C-H1···O1	135.8
AMP-ALA	C-H3···O	153.1
	C-H2···O	144.0
	C-N···H1	110.4
AMP-ALA-IND	C-H6···O4	161.6
	C-H5···O4	134.5
	C-N···H3	110.3
	C-H4···O3	95.9
	C-O2···H2	94.3
	C-O1···H2	99.2
	C-O1···H1	127.9
AMP-ALA-DFO	C-N2···H3	78.5
	C-O1···H2	108.5
	C-N1···H2	91.5
	C-N1···H1	134.1
	C-H6···O2	151.3
	C-H5···O2	144.6
	C-N3···H4	111.4

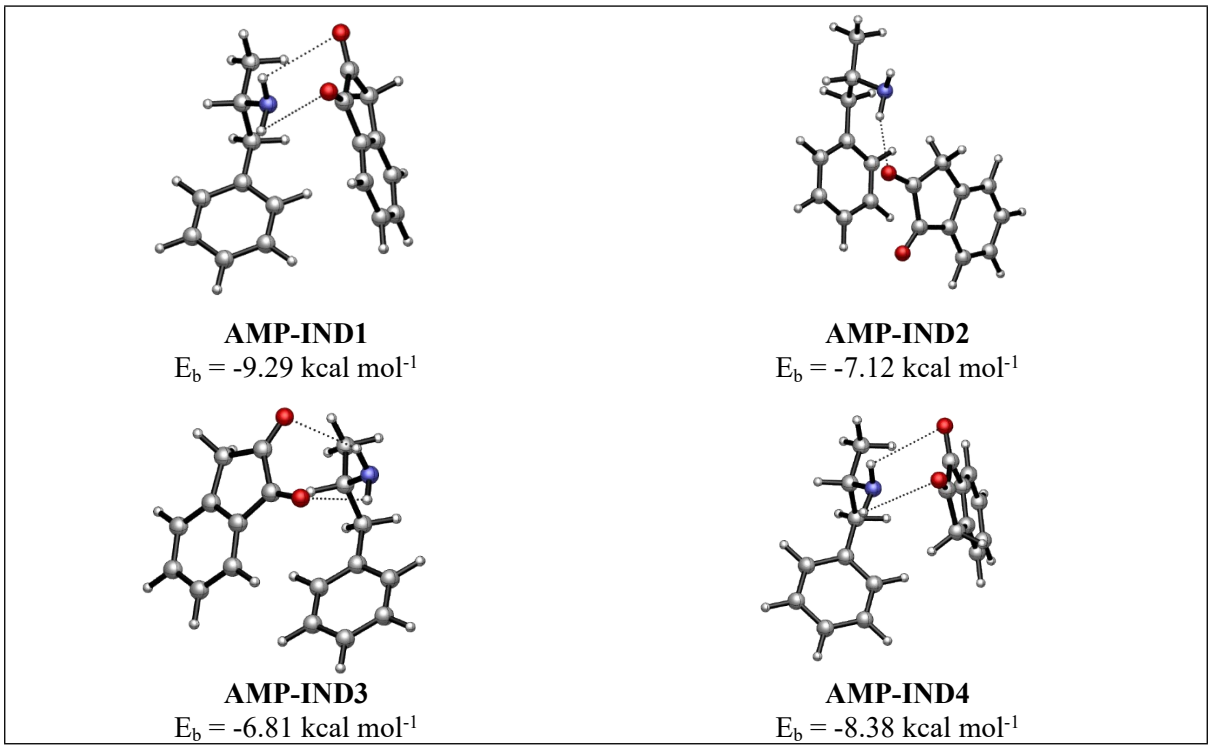

Fig. S2 Optimised geometries of AMP binding with IND

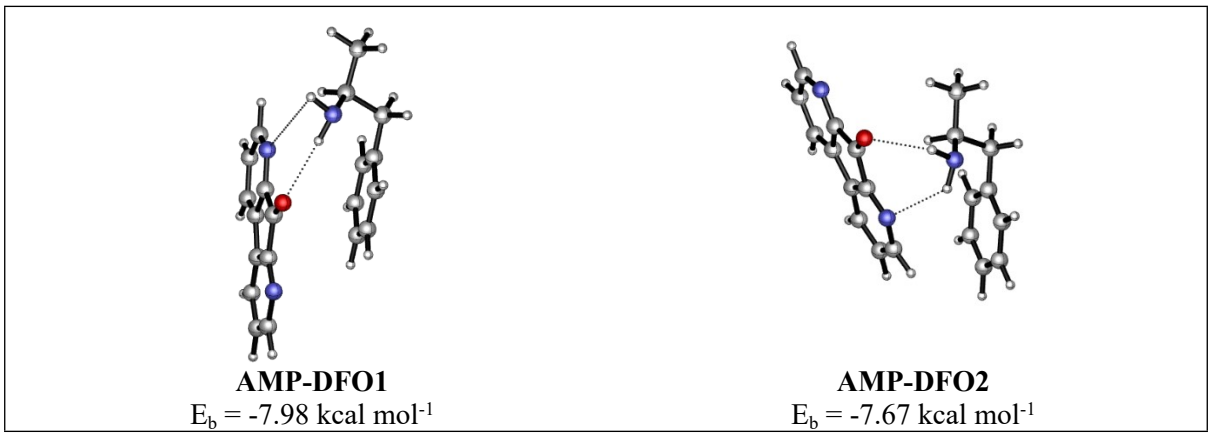

Fig. S3 Optimised geometries of AMP binding with DFO

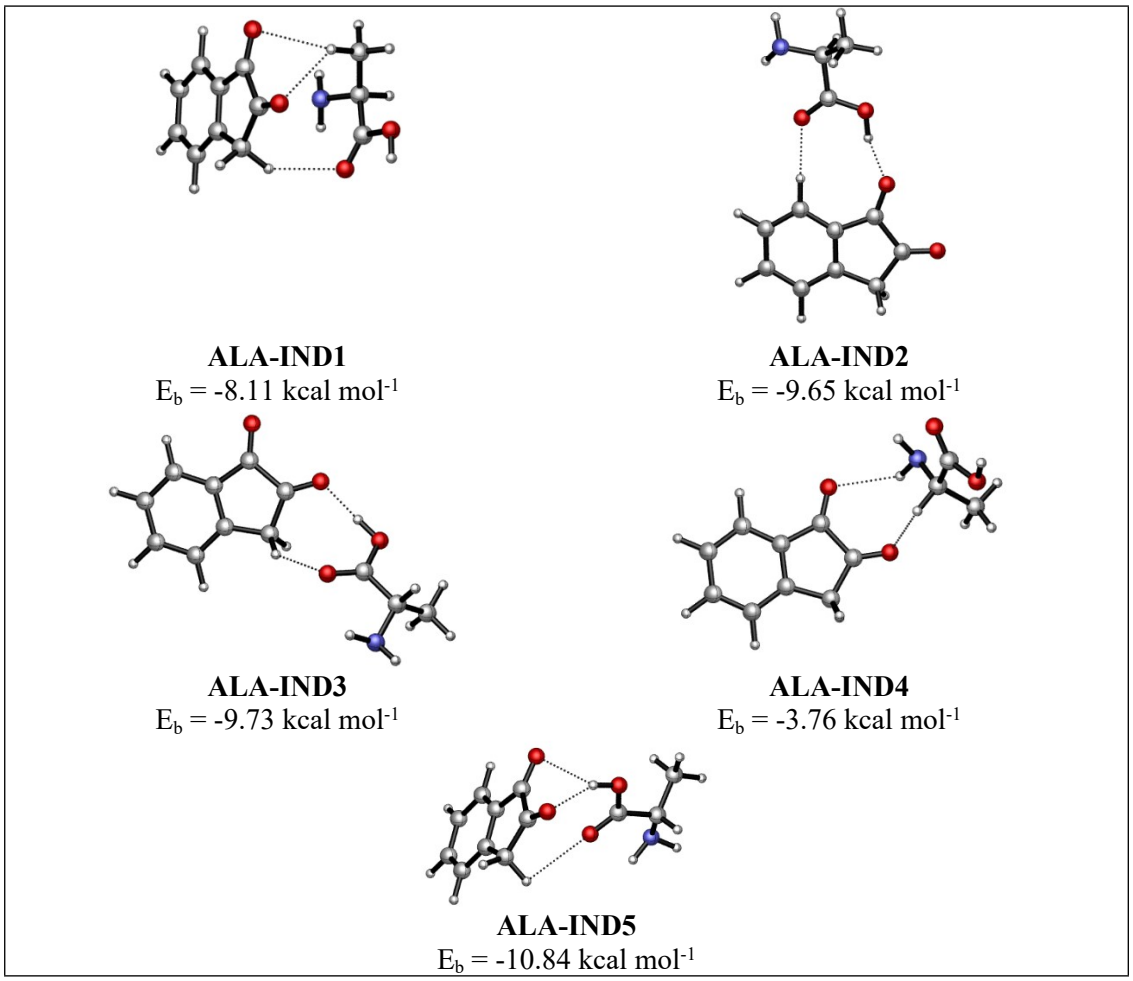

Fig. S4 Optimised geometries of ALA binding with IND

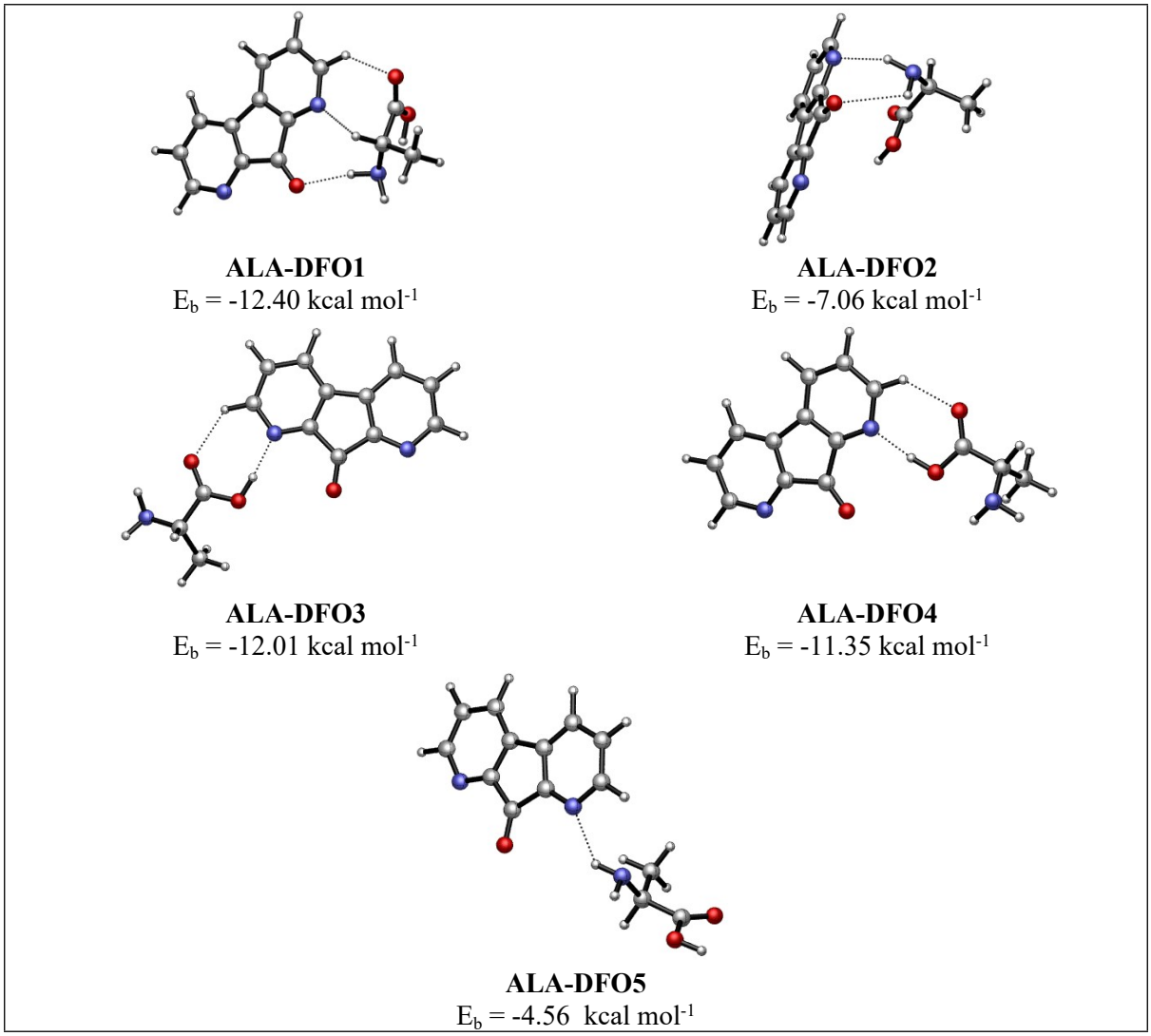

Fig. S5 Optimised geometries of ALA binding with DFO

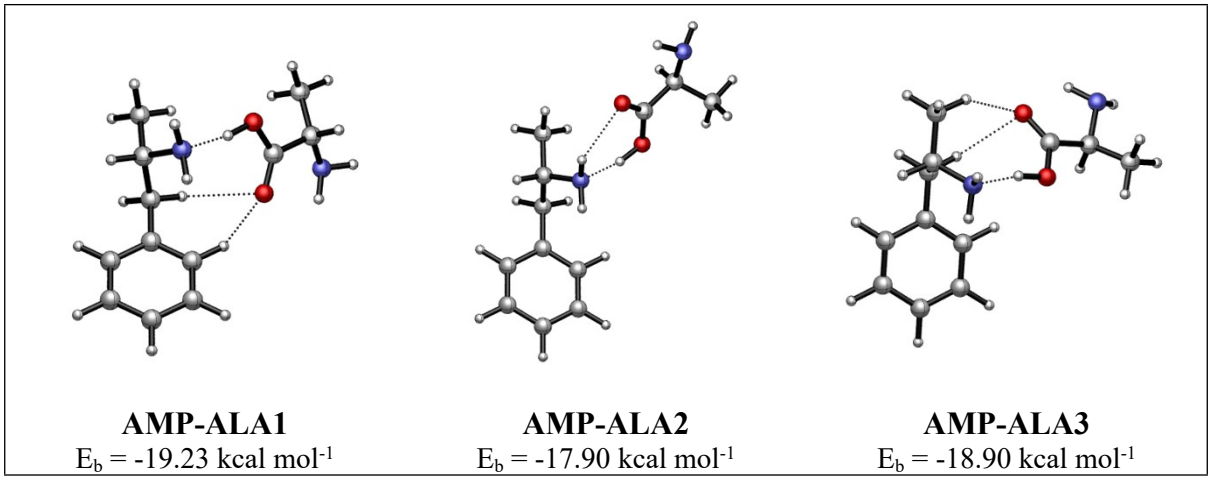

Fig. S6 AMP binding with ALA

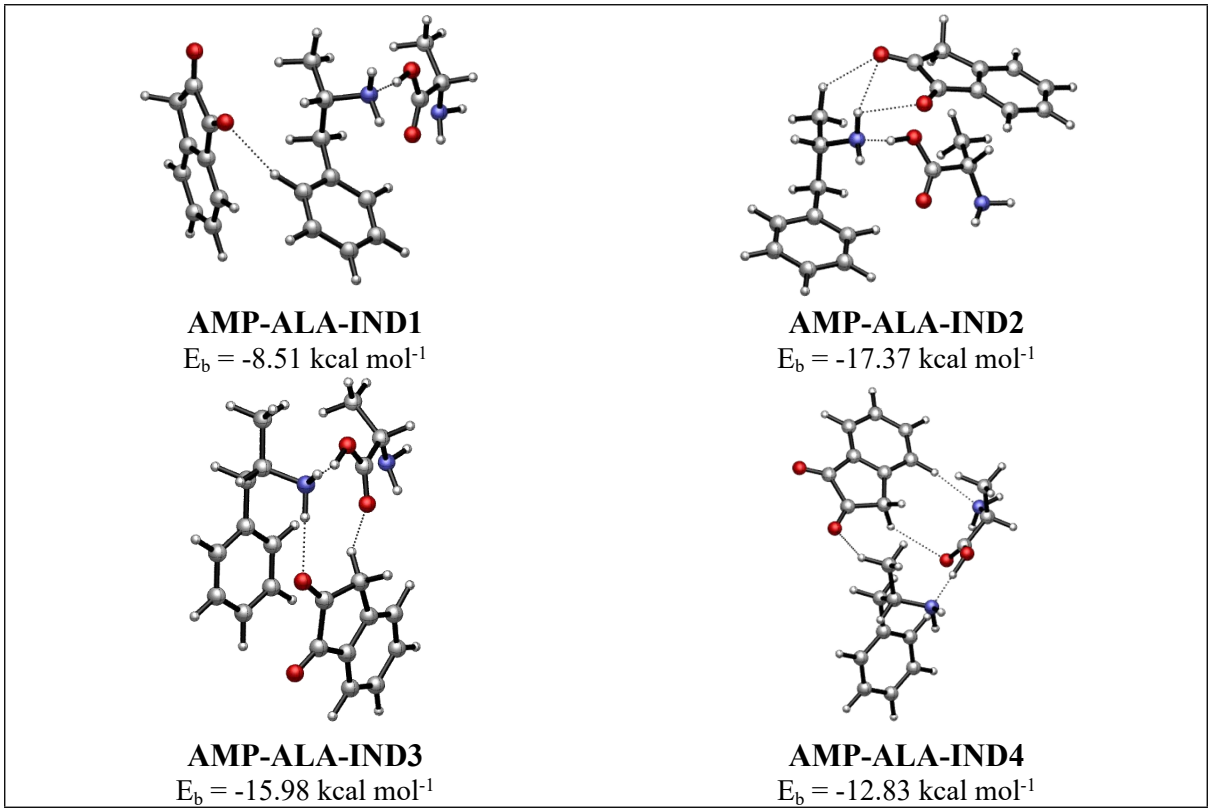

Fig. S7 Optimised geometries of AMP-ALA binding with IND

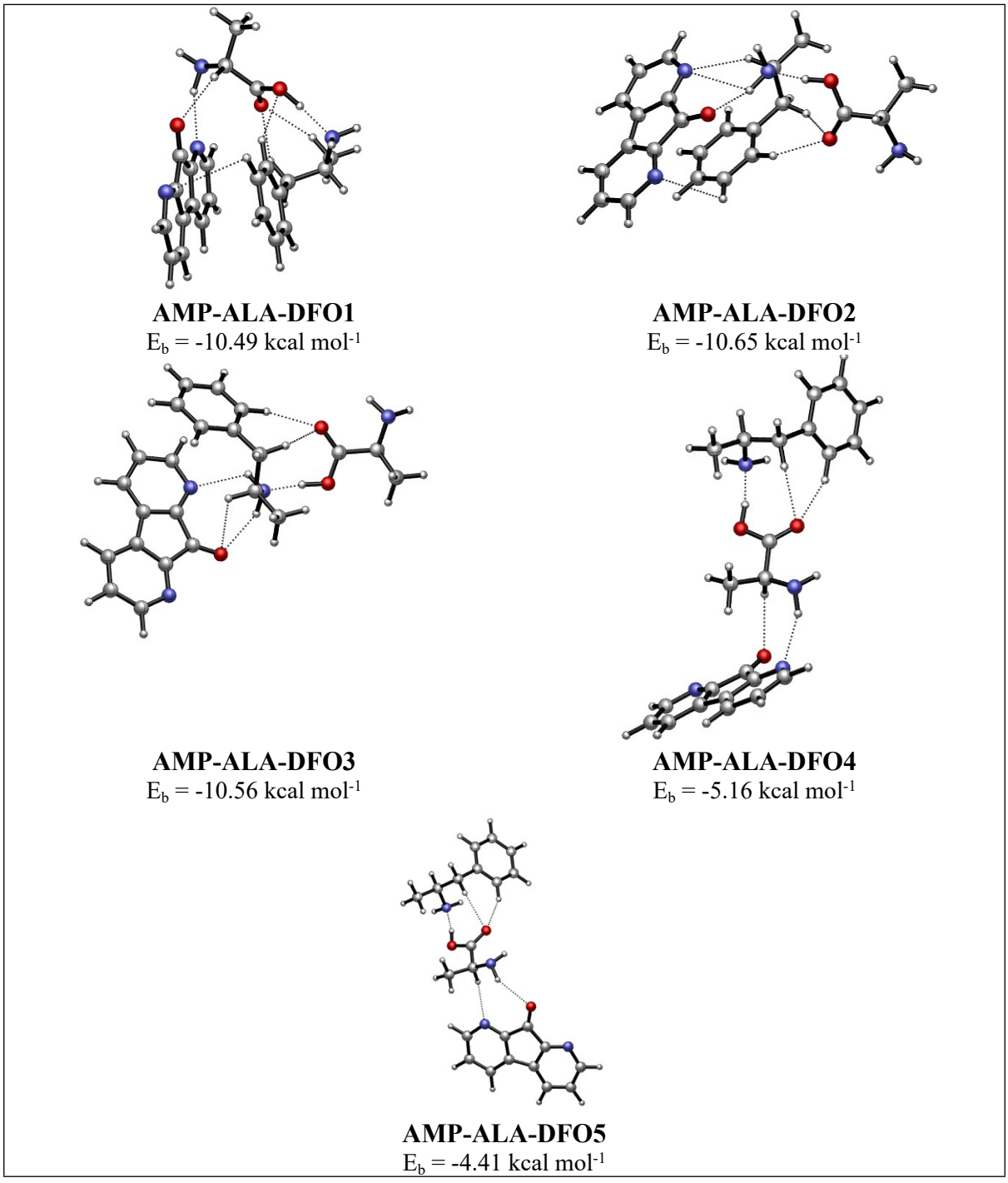

Fig. S8 Optimised geometries of AMP-ALA binding with DFO

Table S2 Uncorrected energies, ZPE and the BSSE corrections of the binding structures

Structure	Energy/ Hartree	ZPE	BSSE corrections	Total Gibbs energy/ Hartree	Total Enthalpy/ Hartree
AMP	-405.5789852	0.203355		-405.4107857	-405.3650843
IND	-497.0278038	0.126506		-496.9358055	-496.8917535
DFO	-607.5196195	0.145809		-607.408872	-607.363528
ALA	-323.7626074	0.107742		-323.696751	-323.6583515
AMP-IND	-902.6299496	0.331688	0.006536312	-902.3473677	-902.2779451
AMP-DFO	-1013.119958	0.350379	0.007421628	-1012.820813	-1012.747751
ALA-IND	-820.8136364	0.2362315	0.003970789	-820.6239913	-820.5598598
ALA-DFO	-931.3104424	0.2564831	0.005523108	-931.1021691	-931.0354064
AMP-ALA	-729.3751204	0.3139828	0.006835885	-729.1086316	-729.0426602
AMP-ALA-IND	-1226.431255	0.4411407	0.007990962	-1226.050716	-1225.961769
AMP-ALA-DFO	-1336.919433	0.4605266	0.006991568	-1336.522433	-1336.42906

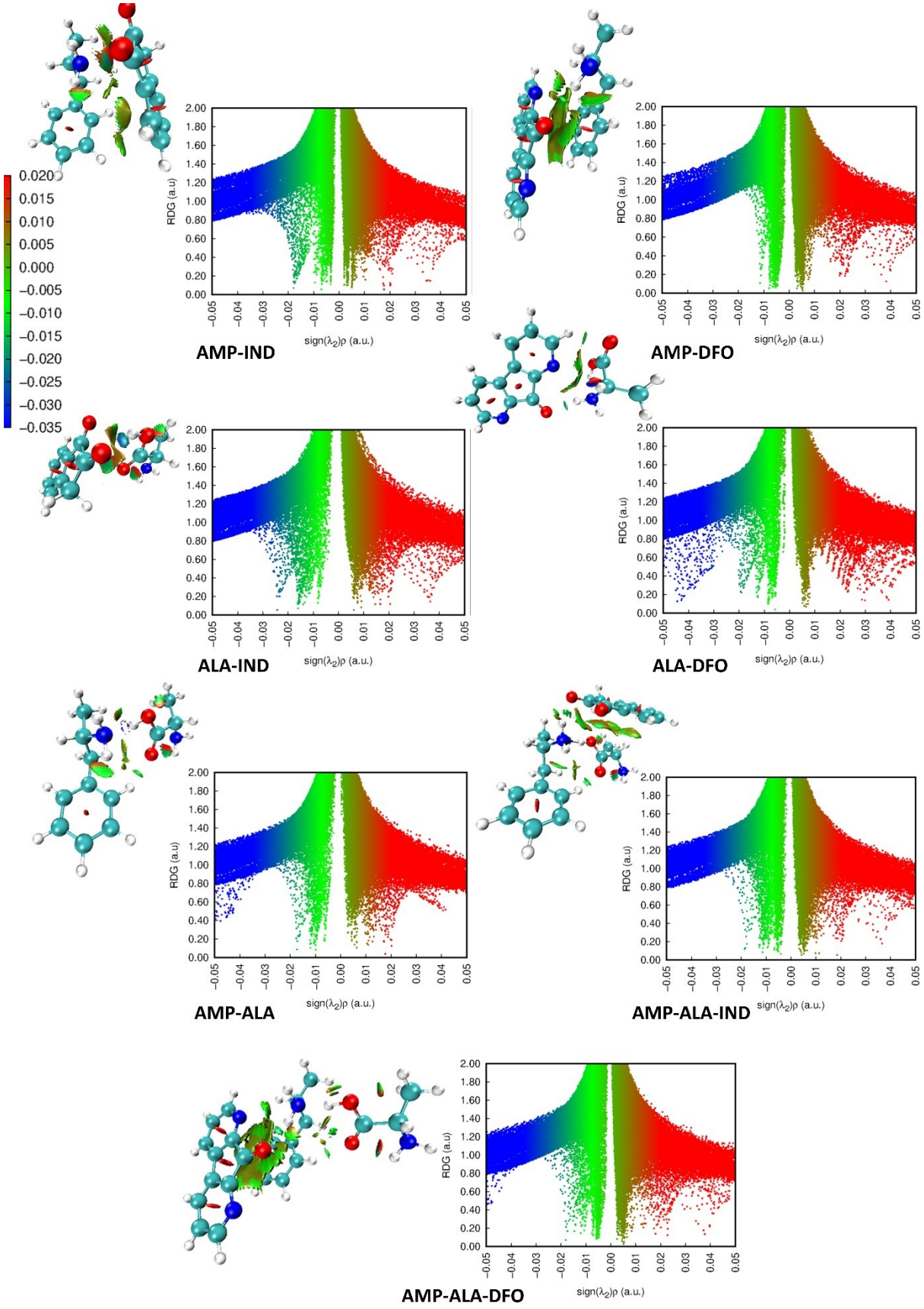

Fig. S9 2D and 3D plots of the binding structures. The NCI isosurfaces correspond to an isovalue of s = 0.5 a.u.

We performed NCI analysis of the binding structures and the 2D and 3D NCI plots are displayed in **Fig. S9**. In the plot for AMP-IND, a blue patch between the NH_2 of AMP and the O of IND shows attractive interaction which spreads over a broad intermolecular space from a value of sign (λ2)ρ of −0.05 to −0.02 a.u. A trough at approximately sign(λ2)ρ = −0.02 a.u. shows the hydrogen bond H···O interaction as depicted by a blue isosurface. Stronger hydrogen bond interactions are depicted as darker blue in the isosurfaces, that is, (λ2)ρ of −0.05 to -0.025 a.u. These interactions are present in ALA-DFO, AMP-ALA and AMP-ALA-DFO. The green isosurfaces (−0.015 > sign (λ2)ρ > 0.005) represent van der Waals interactions between the molecules. In the 0 > sign (λ2)ρ > 0.01 region, the repulsive interactions are depicted by brown isosurfaces. Finally, the aromatic rings region of AMP, IND and DFO cause steric repulsions shown by the red region at sign (λ2)ρ = 0.010 to 0.020 a.u. Similar isosurfaces were observed in all the other binding structures.

Table S3 Values of SAPT components and TSAPT0 [kcal mol^{-1}]

Structure	***El***	***Ex***	***I***	***D***	T_{SAPT0}
AMP-IND	-16.42	23.21	-4.23	-13.46	-10.91
AMP-DFO	-9.62	17.33	-2.49	-16.69	-11.47
ALA-IND	-18.55	18.71	-5.78	-7.45	-13.07
ALA-DFO	-15.45	12.65	-4.15	-6.67	-13.63
AMP-ALA	-30.26	35.87	-13.92	-8.30	-16.61
AMP-ALA-IND	-15.48	18.89	-3.53	-13.77	-13.90
AMP-ALA-DFO	-11.85	18.69	-2.93	-17.19	-13.29

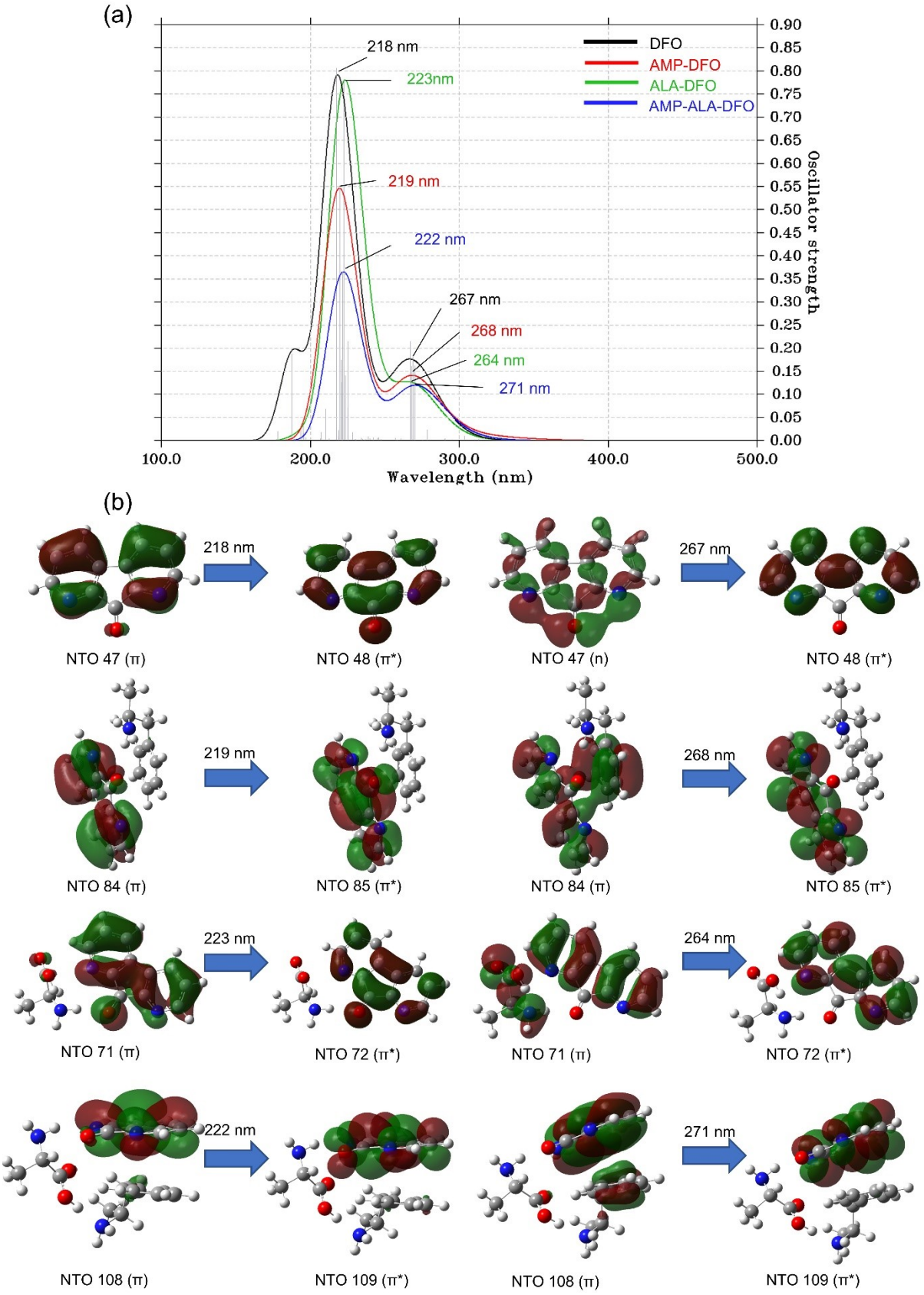

Fig. S10 (a) Computed UV-Vis spectra of DFO, AMP-DFO, ALA-DFO and AMP-ALA-DFO using the TD-DFT/ CAM-B3LYP/6-31+G(d,p) method. **(b)** The dominant natural transition orbital (NTO) pairs at the corresponding calculated λmax.

Table S4 Computed absorption wavelengths (λmax), oscillator strengths (f), excitation energies (Ex), major molecular orbital (MO) assignments of the structures under study in the gas phase at the TD-DFT/CAM-B3LYP/6-31+G(d,p) level of theory

Structures	State	λ_{max} /nm	*f*	*Ex /eV*	Major MO assignments
IND	S4	172	0.19	4.84	H-2 → L (91.4%)
	S11	259	0.43	7.05	H-1 → L+2 (53.2%),
					H-2 → L+1 (33.2%)
AMP-IND	S5	187	0.14	5.04	H-5 → L (65.1%), H-2 → L (17.8%), H-4 → L (7.6%)
	S20	249	0.15	6.75	H-2 → L+1 (35.3%),
					H-2 → L+3 (8.2%)
ALA-IND	S4	176	0.19	4.77	H-3 → L (91.0%)
	S20	261	0.22	7.17	H-3 → L+2 (70.2%),
					H-2 → L+1 (10.6%)
AMP-ALA-IND	S6	199	0.14	4.79	H-6 → L (69.9%), H → L (9.5%),
					H-7 → L (8.4%)
	S19	262	0.14	6.30	H-5 → L+1 (79.7%),
					H-6 → L+2 (7.6%)
DFO	S5	187	0.21	4.64	H → L+1 (79.9%), H-5 → L (14.7%)
	S10	218	0.81	5.70	H-5 → L (78.0%), H → L+1 (16.9%)
	S16	267	0.19	6.62	H-3 → L+1 (48.3%),
					H → L+5 (25.3%), H → L+2 (13.2%)
AMP-DFO	S8	219	0.18	4.61	H-3 → L+1 (55.8%),
					H-2 → L+1 (21.1%), H-8 → L (12.8%)
	S17	268	0.55	5.65	H-8 → L (70.7%), H-3 → L+1 (12.7%), H-6 → L (5.7%)
ALA-DFO	S6	223	0.16	4.63	H-1 → L+1 (42.4%),
					H → L+1 (32.5%), H-7 → L (17.9%)
	S12	264	0.78	5.58	H-7 → L (66.5%), H → L+1 (14.9%), H-6 → L (7.0%)
AMP-ALA-DFO	S8	222	0.16	4.59	H-1 → L+1 (56.7%),
					H-2 → L+1 (19.1%), H-10 → L (8.2%)
	S17	271	0.37	5.59	H-10 → L (39.1%),
					H-2 → L+1 (14.8%), H-8 → L (11.2%)

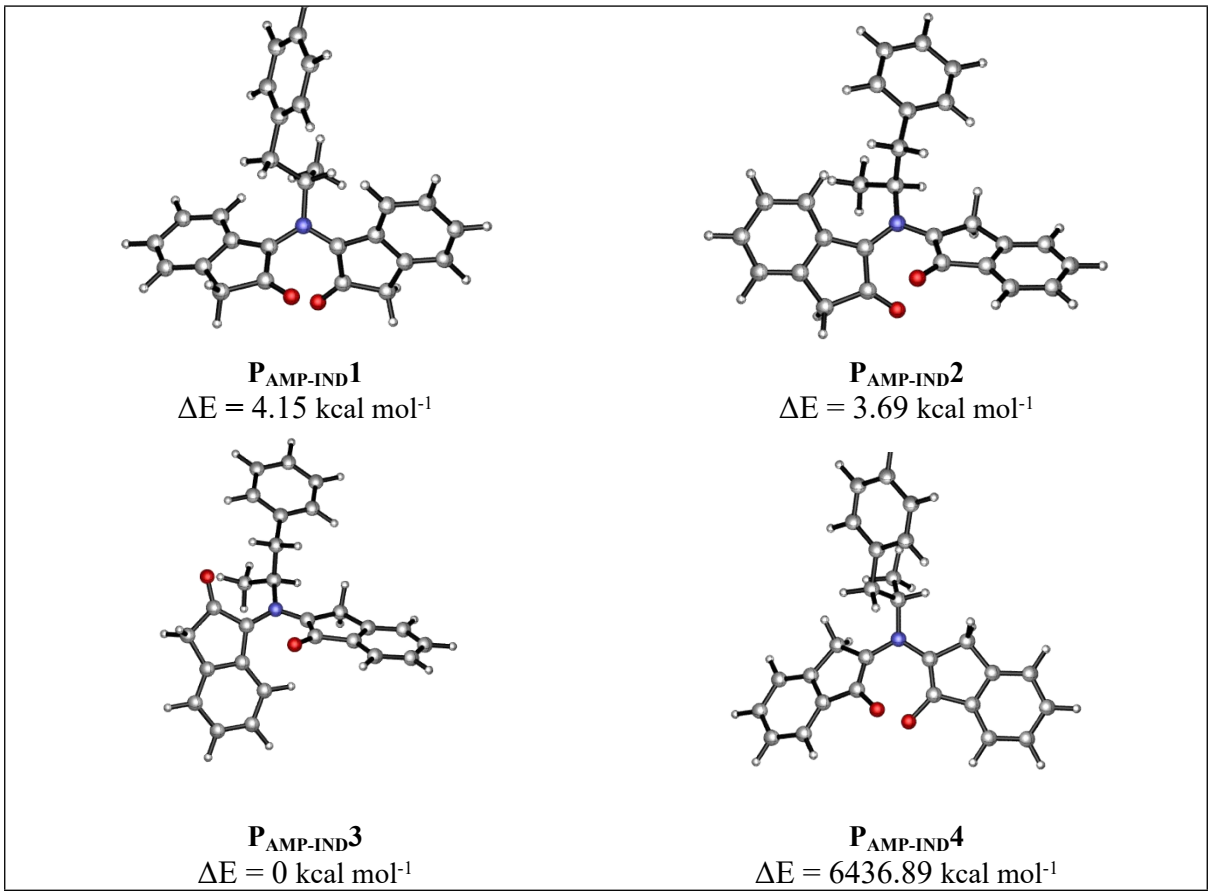

Fig. S11 Optimised geometries and relative stabilities of reaction products between AMP and IND

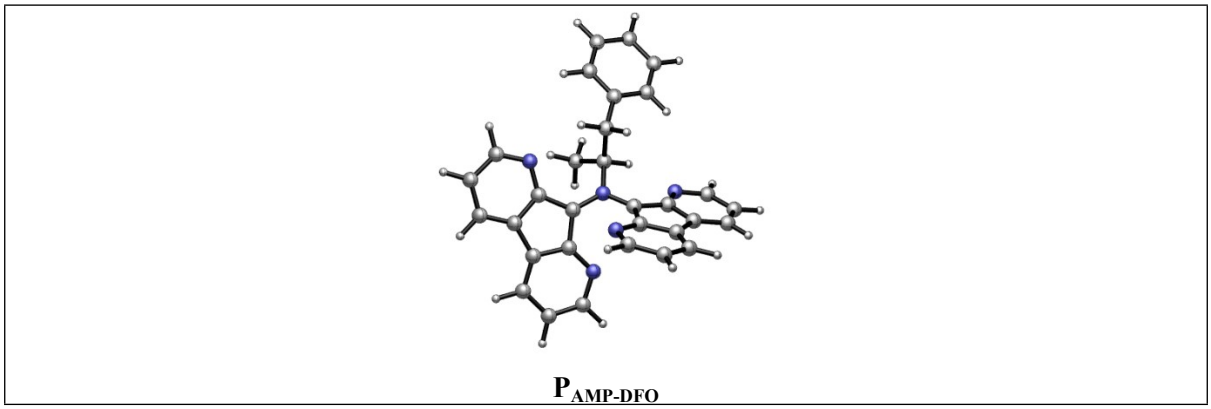

Fig. S12 Optimised geometry of reaction product between AMP and DFO

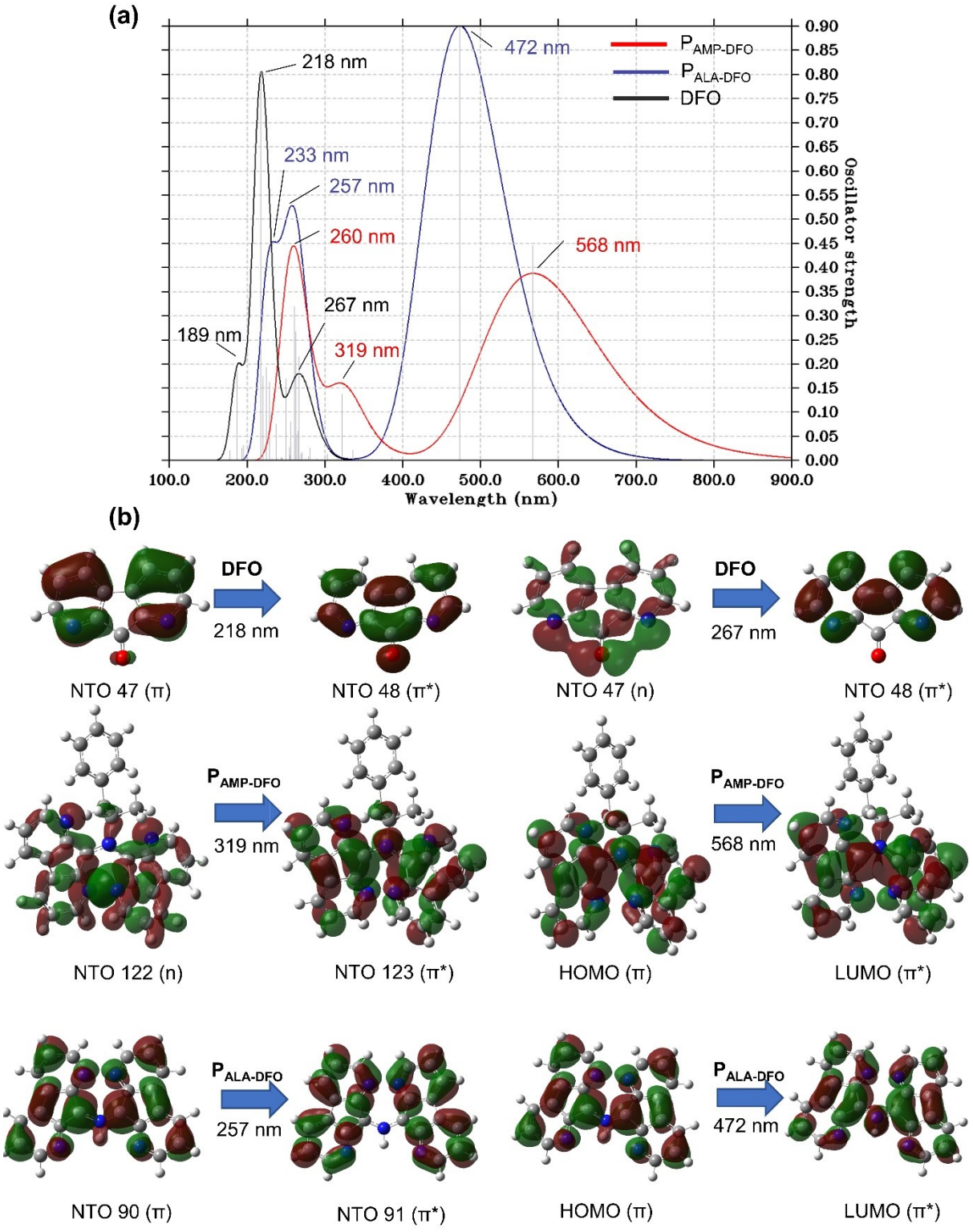

Fig. S13 (a) Computed UV-Vis spectra of DFO, PAMP-DFO and PALA-DFO using the TD-DFT/ CAM-B3LYP/6-31+G(d,p) method. **(b)** The FMOs and dominant natural transition orbital (NTO) pairs at the corresponding calculated λmax

Table S5 Computed absorption wavelengths (λ_{max}), oscillator strengths (*f*), excitation energies (E_x), major molecular orbital (MO) assignments of the structures under study in the gas phase at the TD-DFT/CAM-B3LYP/6-31+G(d,p) level of theory

Structures	State	λ_{max} /nm	*f*	*Ex* /eV	Major MO assignments
IND	S4	172	0.19	4.84	H-2 → L (91.4%)
	S11	259	0.43	7.05	H-1 → L+2 (53.2%),
					H-2 → L+1 (33.2%)
$P_{AMP-IND}$	S1	511	0.31	2.41	H → L (94.7%)
	S11	253	0.20	5.09	H → L+6 (76.7%)
$P_{ALA-IND}$	S1	469	0.58	2.64	H → L (101.7%)
	S9	251	0.35	4.97	H → L+3 (52.9%), H-4 → L (25.9%), H-1 → L (9.9%)
	S18	188	0.18	6.67	H-3 → L+1 (17.0%), H-7 → L (15.6%), H-4 → L+2 (13.1%)
DFO	S5	187	0.21	4.64	H → L+1 (79.9%), H-5 → L (14.7%)
	S10	218	0.81	5.70	H-5 → L (78.0%), H → L+1 (16.9%)
	S16	267	0.19	6.62	H-3 → L+1 (48.3%),
					H → L+5 (25.3%), H → L+2 (13.2%)
$P_{AMP-DFO}$	S1	568	0.45	2.18	H → L (98.1%)
	S6	319	0.14	3.84	H-5 → L (87.5%)
	S14	260	0.27	4.71	H-2 → L+1 (21.0%),
					H → L+3 (18.2%), H-11 → L (15.9%)
$P_{ALA-DFO}$	S1	472	0.90	2.58	H → L (101.0%)
	S12	257	0.29	4.74	H → L+3 (22.9%), H-8 → L (21.0%), H-2 → L+1 (20.2%),
					H-1 → L+2 (17.8%)
	S20	233	0.32	5.50	H-8 → L (45.2%)

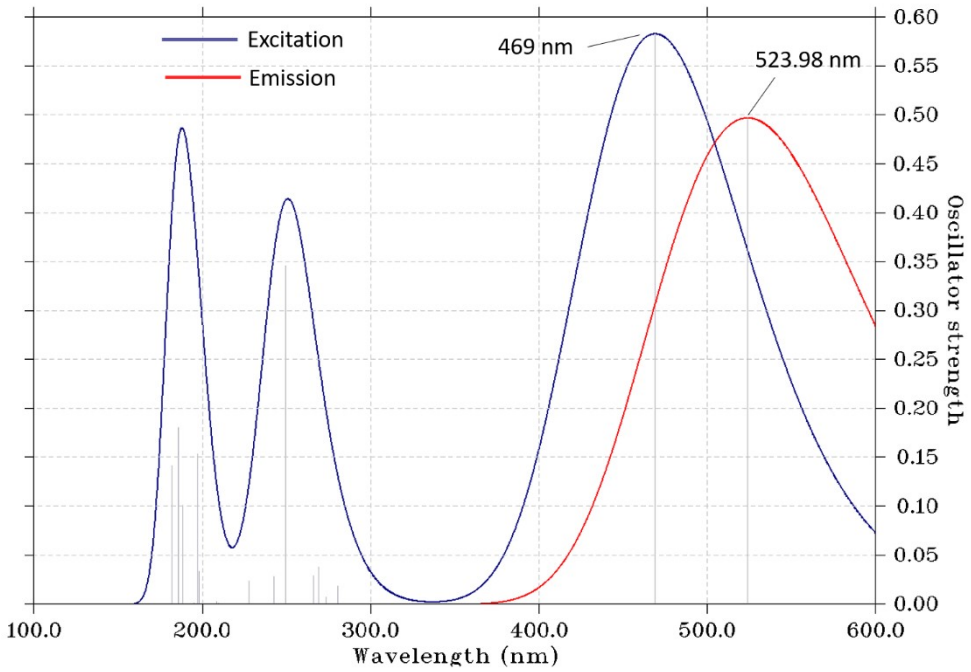

Fig. S14 Excitation and fluorescence spectra for $P_{ALA\text{-}IND}$

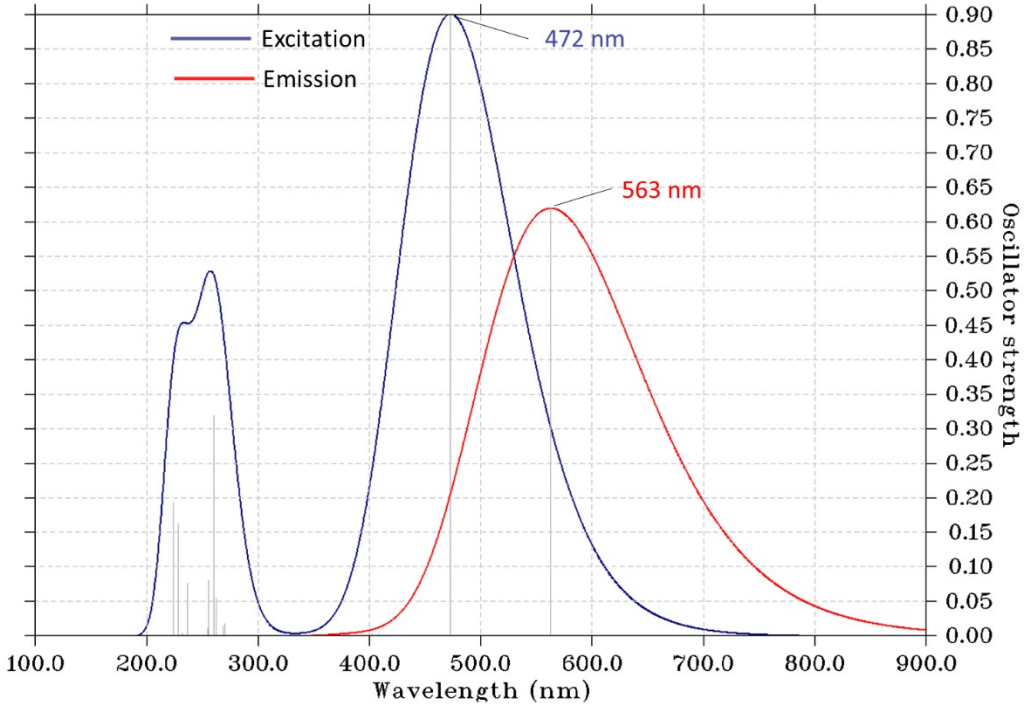

Fig. S15 Excitation and fluorescence spectra for $P_{ALA\text{-}DFO}$

The first singlet excited states (S_1) of $P_{ALA\text{-}IND}$ and $P_{ALA\text{-}DFO}$ were analysed using TD-DFT method. We optimised the ground state structures using the TD-CAM-B3LYP method with the 6-31G(d) basis set.[1] Subsequently, the fluorescence spectra were simulated using the Multiwfn program[2] as shown in **Fig. S14** and **Fig. S15**.

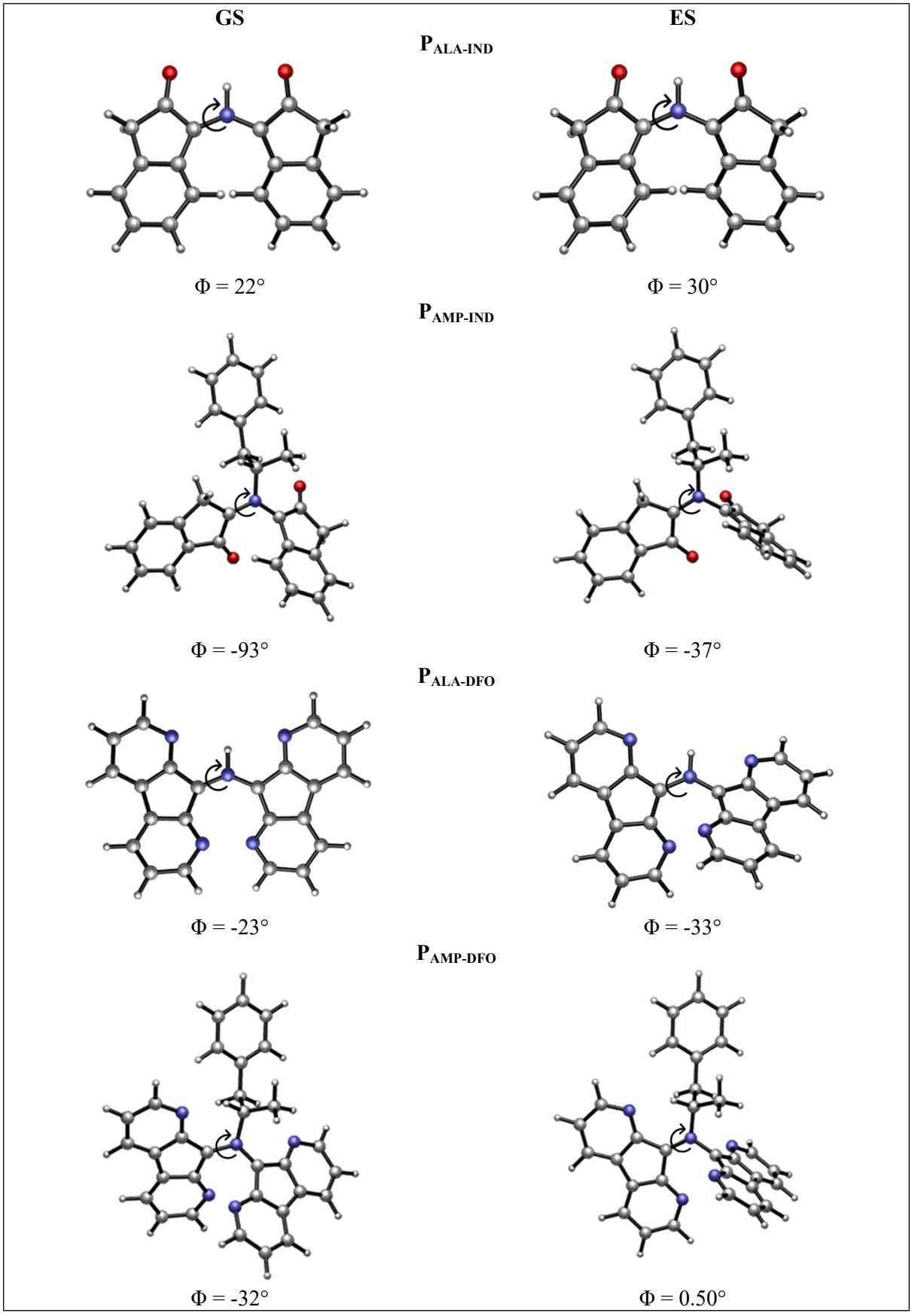

Fig. S16 Ground state (GS) and excited state (ES) geometries of $P_{ALA-IND}$, $P_{ALA-DFO}$, $P_{AMP-IND}$ and $P_{AMP-DFO}$

Coordinates of optimised geometries of AMP, ALA, IND and DFO

AMP

C	-3.050543000	0.100683000	-0.323148000
C	-2.416029000	-1.135007000	-0.468352000
C	-1.087973000	-1.290613000	-0.071420000
C	-0.368957000	-0.219866000	0.478541000
C	-1.017785000	1.015278000	0.618388000
C	-2.346593000	1.175890000	0.221140000
H	-4.085607000	0.222789000	-0.628676000
H	-2.957258000	-1.978722000	-0.887364000
H	-0.599784000	-2.255821000	-0.184497000
H	-0.469944000	1.854391000	1.038491000
H	-2.832249000	2.140366000	0.340438000
C	1.085950000	-0.382071000	0.856440000
C	2.047383000	-0.165598000	-0.333136000
H	1.355408000	0.333365000	1.641672000
N	1.914301000	1.215635000	-0.813635000
H	2.530494000	1.360565000	-1.610475000
H	0.966986000	1.370472000	-1.152051000
H	1.254515000	-1.389392000	1.255451000
C	3.497395000	-0.407918000	0.088962000
H	3.631925000	-1.426683000	0.466608000
H	4.180885000	-0.271886000	-0.757024000
H	3.785618000	0.300274000	0.872429000
H	1.781811000	-0.913831000	-1.104052000

ALA

C	0.680495000	0.022524000	0.365487000
N	1.387082000	-1.169037000	-0.092978000
H	2.267378000	-1.262904000	0.404188000
H	0.826018000	-1.995220000	0.095961000

C	-0.797817000	-0.138580000	0.033212000
O	-1.340798000	-1.190053000	-0.228180000
O	-1.474784000	1.030070000	0.122833000
H	-2.405795000	0.818315000	-0.059347000
C	1.295076000	1.281410000	-0.259663000
H	2.350977000	1.350393000	0.019814000
H	1.237292000	1.223173000	-1.349608000
H	0.784376000	2.184067000	0.082001000
H	0.688305000	0.153175000	1.466394000

IND

C	-1.693257000	-1.411686000	0.000163000
C	-0.411292000	-0.866757000	0.000164000
C	-0.251832000	0.529497000	-0.000006000
C	-1.349788000	1.395115000	-0.000178000
C	-2.627224000	0.845027000	-0.000169000
C	-2.792951000	-0.549418000	-0.000001000
H	-1.838999000	-2.488055000	0.000284000
H	-1.185218000	2.468175000	-0.000309000
H	-3.500621000	1.489724000	-0.000295000
H	-3.796236000	-0.965683000	-0.000005000
C	1.175279000	0.891789000	-0.000008000
C	0.916183000	-1.592416000	0.000316000
O	1.687888000	1.992385000	-0.000203000
C	1.951296000	-0.462325000	0.000136000
O	3.152617000	-0.573244000	0.000049000
H	1.058445000	-2.230091000	0.880898000
H	1.058483000	-2.230464000	-0.879984000

DFO

C	3.366097000	0.021054000	-0.000003000
C	3.025240000	-1.336748000	-0.000011000

C	1.678546000	-1.714431000	-0.000006000
C	0.737606000	-0.691142000	0.000009000
C	1.194659000	0.642136000	0.000017000
N	2.467348000	1.020485000	0.000011000
H	1.388205000	-2.761023000	-0.000016000
H	4.412040000	0.318758000	-0.000008000
H	3.809921000	-2.086457000	-0.000023000
C	-1.194659000	0.642136000	0.000017000
C	-0.737606000	-0.691142000	0.000009000
C	-1.678546000	-1.714431000	-0.000006000
C	-3.025240000	-1.336748000	-0.000011000
C	-3.366097000	0.021054000	-0.000003000
N	-2.467348000	1.020485000	0.000011000
H	-1.388205000	-2.761023000	-0.000016000
H	-3.809921000	-2.086457000	-0.000023000
H	-4.412040000	0.318758000	-0.000008000
C	0.000000000	1.574673000	0.000048000
O	0.000000000	2.784023000	-0.000051000

References:

1 L. M. Hunnisett, P. F. Kelly, S. Bleay, F. Plasser, R. King, B. McMurchie and P. Goddard, *J. Chem. Phys.*, 2021, **154**, 1–5.

2 T. Lu and F. Chen, *J. Comput. Chem.*, 2012, **33**, 580–592.